Supplement of Clim. Past, 20, 1365–1385, 2024
https://doi.org/10.5194/cp-20-1365-2024-supplement

Supplement of

Investigating similarities and differences of the penultimate and last glacial terminations with a coupled ice sheet–climate model

Aurélien Quiquet and Didier M. Roche

Correspondence to: Aurélien Quiquet (aurelien.quiquet@lsce.ipsl.fr)

Table S1. Main parameters of the GRISLI-iLOVECLIM coupled model. While many other parameters exist in the model, this small subset corresponds to the one that are often used as tunable parameters of the coupled model. Their values are identical to the one used in Quiquet et al. (2021).

Parameter	Description	Value
λ ($\mathrm{W\,m^{-2}\,K^{-1}}$)	Melt coefficient for the surface mass balance model	10
c_{rad} ($\mathrm{W\,m^{-2}}$)	Melt coefficient for the surface mass balance model	-40
$bias_f$ ($^{\circ}\mathrm{C}^{-1}$)	For local c_{rad} change, $c'_{rad} = c_{rad} \times (1 + bias_f * T_{bias})$	0.1
F_g (-)	Melt coefficient for the sub-shelf melt model	15×10^{-3}
E_f (-)	Ice flow enhancement factor	1.8
C_f $\mathrm{Pa\,yr\,m^{-1}}$	Basal friction coefficient	1.58×10^{-3}

S1: elaboration of alternative ice sheet geometries for the penultimate glacial maximum

In the standard version of the model, the melt parameter c_{rad} used in the surface mass balance model is locally changed according to the annual mean temperature bias with respect to present-day reanalysis ERA-interim. The local modification is linear, using a coefficient of $0.1^{\circ}\mathrm{C}^{-1}$. This has been implemented to indirectly correct for the temperature biases in the climate model. For a temperature bias of +10°C we use a c_{rad} of -80 $\mathrm{W\,m^{-2}}$ instead of the reference value of -40 $\mathrm{W\,m^{-2}}$.

To elaborate alternative ice sheet geometries for the penultimate glacial maximum, we run 100-yr long simulations of the climate model with prescribed LGM ice sheets branched from the 142 ka climate equilibrium. For these simulations we modify regionally the value of the reference temperature bias in order to impact the value of the local melt parameter value. For the two alternative ice sheet geometries, we divide by 5 the temperature bias in the region of North America (approximatively for longitudes from -140 to 0 °E). Since the temperature bias is mostly positive in this region, this modification results in higher value of the c_{rad} parameter (more melt). For Eurasia (longitude lower to about 140 °E), we replace the temperature bias by a value of +20 °C (larger Eurasian ice sheet case) and +40 °C (much larger Eurasian ice sheet case). These modifications in Eurasia produce a larger SMB. Finally, we use the climatological SMB resulting from these 100-yr long simulations to force offline the ice sheet model until equilibrium, similarly to what we did to generate the initial LGM ice sheets.

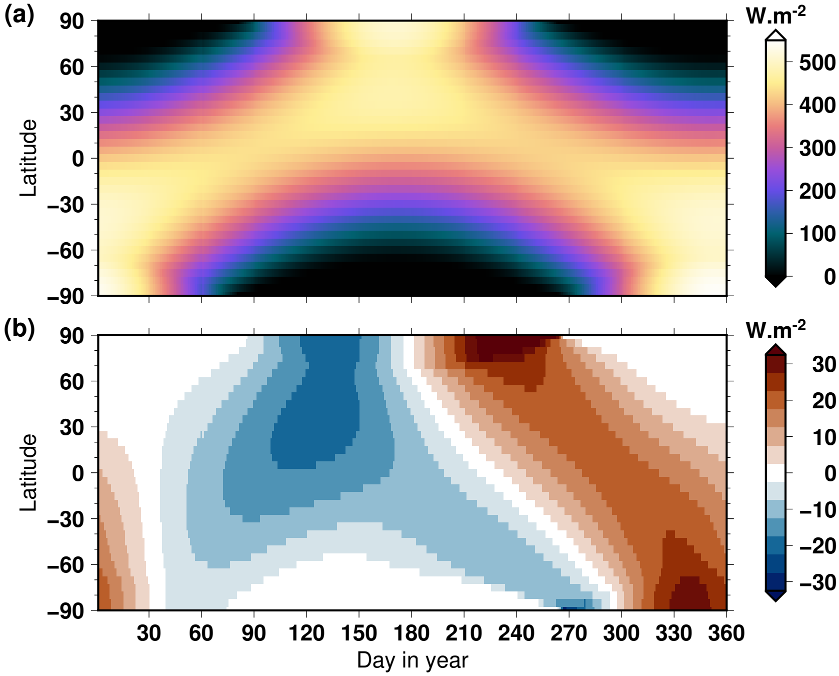

Figure S1. Insolation for the glacial spinup experiments. Daily insolation at 21 ka for the LGM experiment **(a)**. Daily anomalies at 140 ka for the PGM experiment, with respect to the LGM **(b)**.

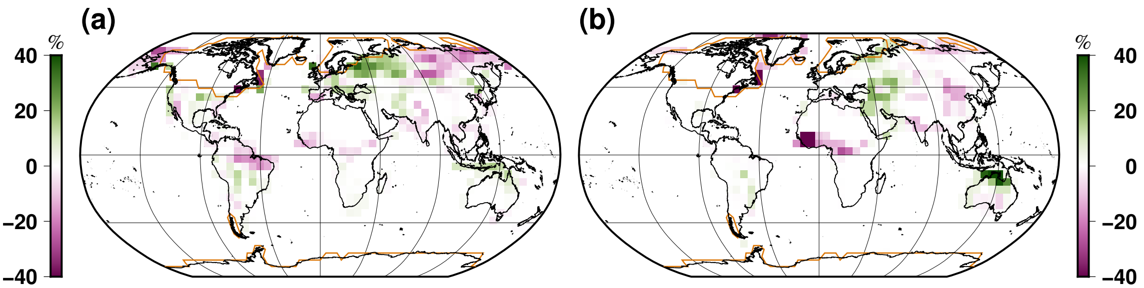

Figure S2. Vegetation fraction for glacial initial conditions. **(a)**: Tree fraction at 26 ka. **(b)**: Tree fraction at 142 ka. **(c)**: Grass fraction at 26 ka. **(d)**: Grass fraction at 142 ka. The orange line is the extent of the ice sheets.

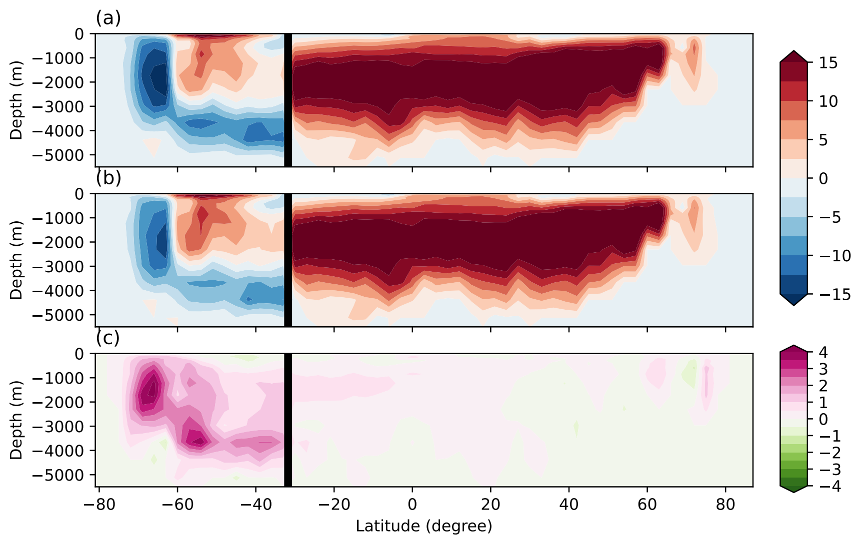

Figure S3. Simulated global (from 81 to 33 °South) and Atlantic stream function (in Sverdrup). At the LGM (21 ka, **a**), at the PGM (142 ka, **b**) and PGM anomaly with respect to the LGM (**c**).

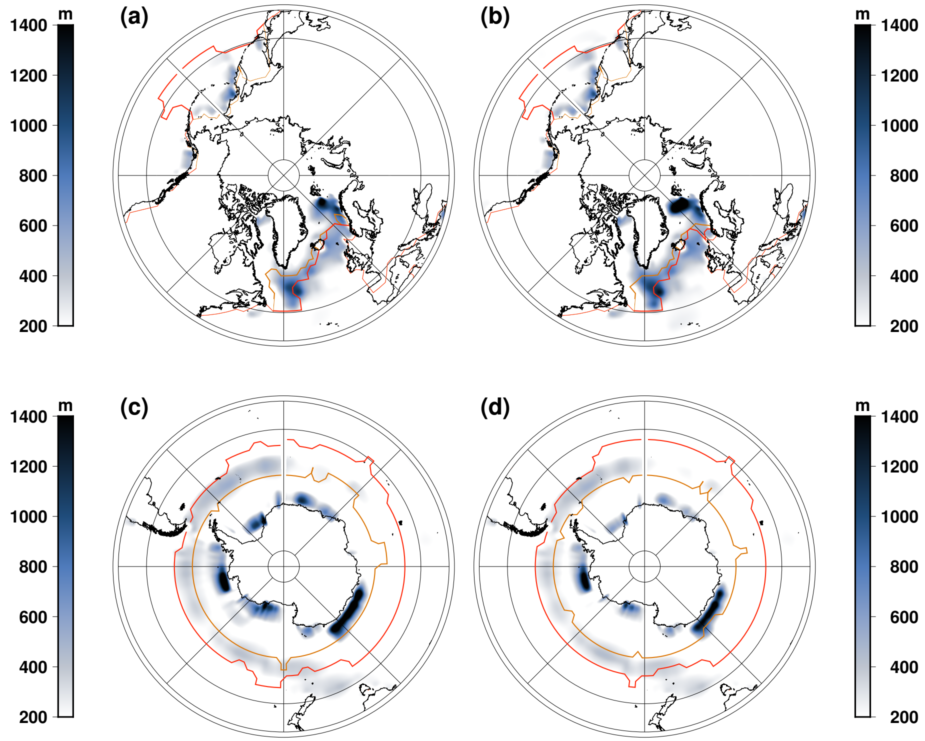

Figure S4. Mixed layer depth for glacial initial conditions. **(a)**: Northern Hemisphere winter (DJF) at 26 ka. **(b)**: Northern Hemisphere winter (DJF) 142 ka. **(c)**: Southern Hemisphere winter (JJA) at 26 ka. **(d)**: Southern Hemisphere winter (JJA) at 142 ka. The red line, respectively orange, stands for the maximal, respectively minimal, sea ice extent.

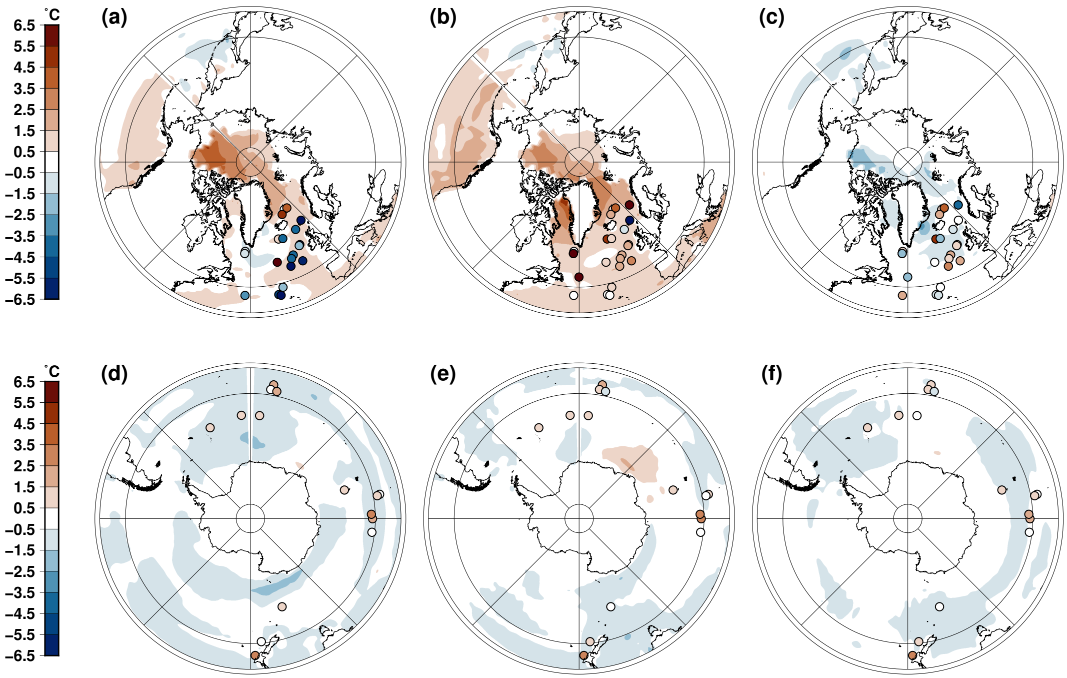

Figure S5. Last interglacial summer sea surface temperature anomalies with respect to the pre-industrial (0 ka). High latitudes anomalies in the Northern Hemisphere (respectively Southern Hemisphere) at 130 ka **(a)** (resp. **(d)**), 125 ka **(b)** (resp. **(e)**) and 120 ka **(c)** (resp. **(f)**). Proxy based reconstructions from Capron et al. (2017) are shown in circles. Summers are defined as the warmest three months. Anomalies are computed with the experiment that does not account for the freshwater flux feedback resulting from ice sheet melting.

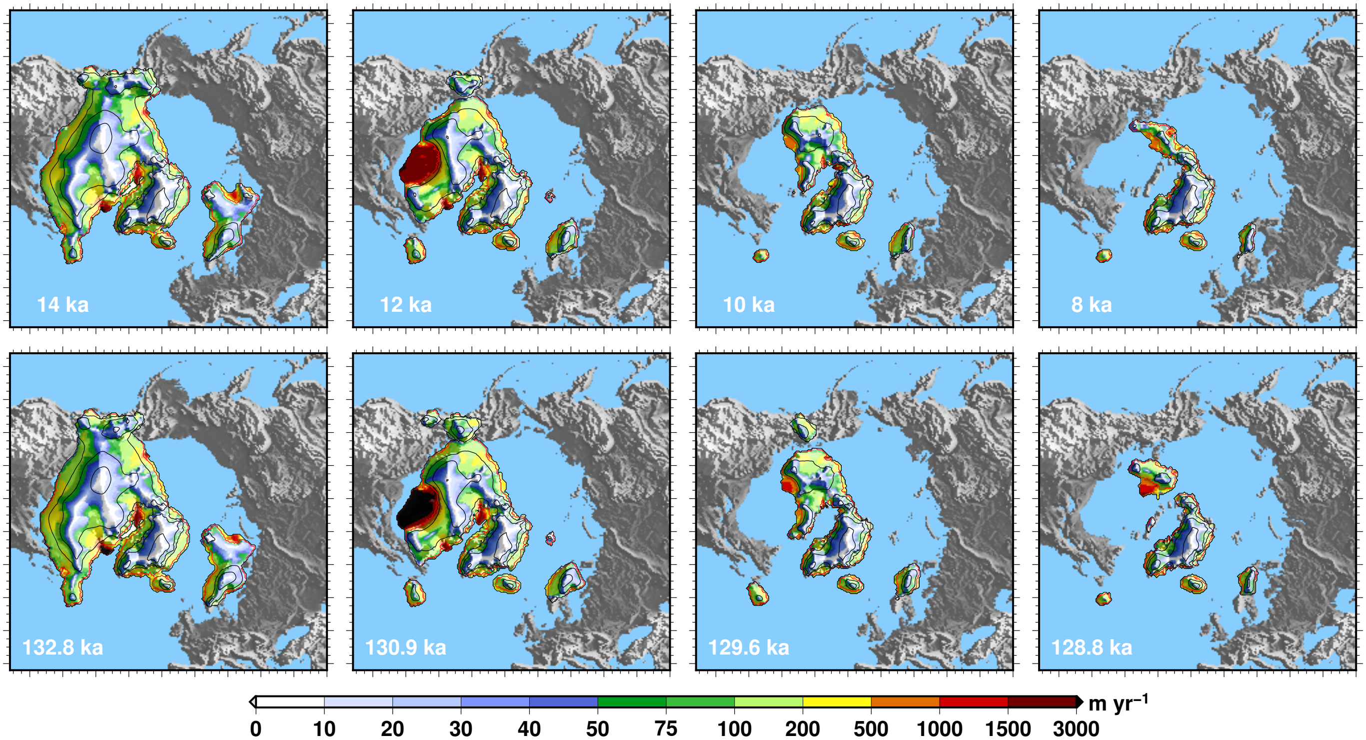

Figure S6. Simulated Northern Hemisphere ice sheets across the two terminations. Four selected snapshots are shown for TI (top) and TII (bottom). The dates for TII have been selected so that the simulated Northern Hemisphere ice volume is equal to the selected dates for TI. The black isocontours show the simulated ice elevation above contemporaneous eustatic sea level (contours separated by 1000 metres). The red contour is the ice sheet grounding line. The colour palette represent the amplitude of the simulated vertically averaged ice sheet velocity, draped over the surface topography. The experiments shown here include the freshwater flux feedback resulting from ice sheet melting.

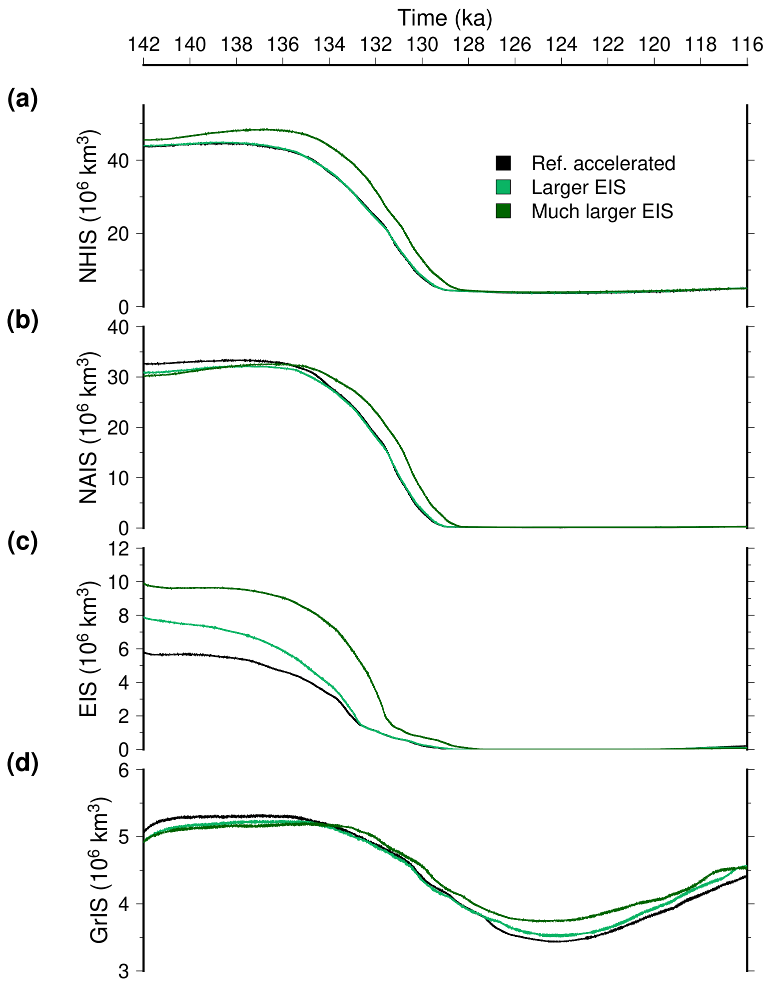

Figure S7. Temporal evolution of individual ice sheet total ice volume across TII using different initial ice sheet geometries. **(a)**: total North Hemisphere ice sheet volume. **(b)**: North American ice sheet volume. **(c)**: Eurasian ice sheet volume. **(d)**: Greenland ice sheet volume. The experiment that uses the reference ice sheet is in black while the experiments with slightly larger (+36 %) and larger (+71 %) Eurasian ice sheet volume are in light and dark green, respectively.

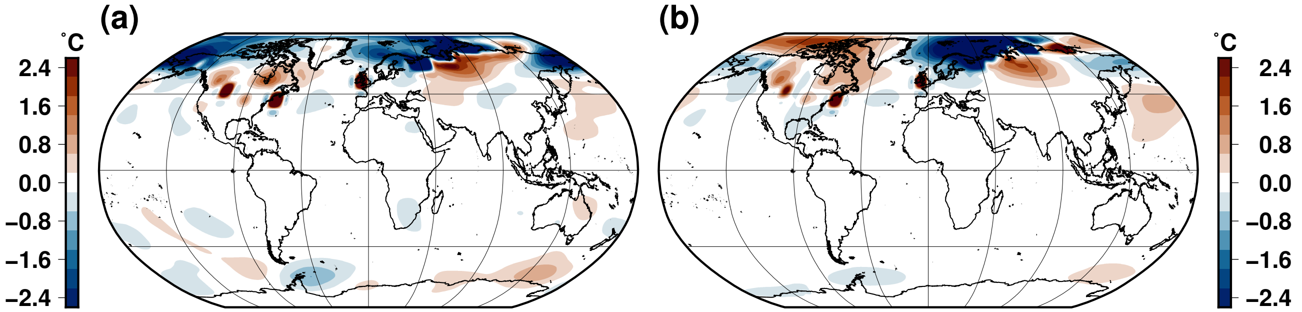

Figure S8. Simulated change in the near surface air temperature at the PGM when using different ice sheets as boundary conditions. **(a)**: Summer JJA temperature difference between the experiment using with the substantially larger (+71 %) Eurasian ice sheet and the reference experiment. **(b)**: Same as **(a)** but for the annual mean temperature.

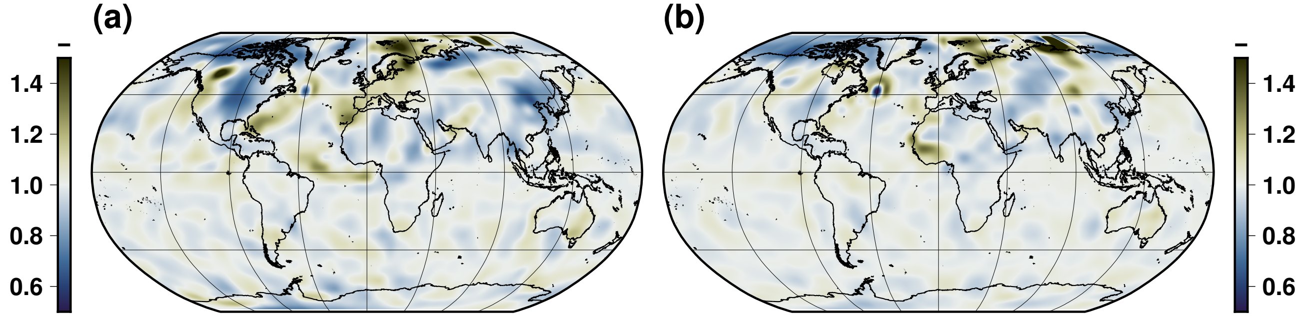

Figure S9. Simulated change in the precipitation at the PGM when using different ice sheets as boundary conditions. **(a)**: Winter DJF precipitation ratio between the experiment using with the substantially larger (+71 %) Eurasian ice sheet and the reference experiment. **(b)**: Same as **(a)** but for the annual mean precipitation.